



# 1-(2-((Z)-6-(2-(Trifluoromethyl)phenyl)hexa-3-en-1,5-diynyl)phenyl)-piperidin-2-one as a new potent apoptosis agent

Yu-Sheng Tu<sup>a</sup>, Tsai-Hui Duh<sup>a</sup>, Chen-Yi Tseng<sup>c</sup>, Ying-Ting Lin<sup>d</sup>, Yu-Hsiang Lo<sup>b</sup>, Yi-Ling Hu<sup>a</sup>, Chen-Hung Chen<sup>a</sup>, Ching-Ming Chien<sup>a</sup>, Sheng-Huei Yang<sup>a</sup>, Shinne-Ren Lin<sup>a</sup>, Shyh-Chyun Yang<sup>b</sup>, Ming-Jung Wu<sup>c,\*</sup>

<sup>a</sup> Faculty of Medicinal and Applied Chemistry, Kaohsiung Medical University, Kaohsiung, Taiwan

<sup>b</sup> Graduate Institute of Pharmaceutical Sciences, Kaohsiung Medical University, Kaohsiung, Taiwan

<sup>c</sup> Department of Chemistry, National Sun Yat-sen University, Kaohsiung, Taiwan

<sup>d</sup> Faculty of Biotechnology, Kaohsiung Medical University, Kaohsiung, Taiwan

## ARTICLE INFO

### Article history:

Received 28 August 2009

Revised 18 September 2009

Accepted 19 September 2009

Available online 25 September 2009

### Keywords:

Acyclic enediynes  
Antitumor agents  
Antitubulin  
Apoptosis

## ABSTRACT

Compounds **4a–f**, **5a–f** and **6–9**, showed significant growth inhibition activity against human tumor cell lines. Of these compounds, 1-(2-((Z)-6-(2-(trifluoromethyl)phenyl)hexa-3-en-1,5-diynyl)phenyl)piperidin-2-one (**8**) displayed the most potent growth inhibition activity. Compound **8** also arrested cancer cells in G2/M phase and induced apoptosis via activation of caspase-3 and -9. According to western-blotting analysis, compound **8** can up-regulate Bax, down-regulate Bcl-2 and XIAP, as well as promote cytochrome *c* release.

© 2009 Elsevier Ltd. All rights reserved.

## 1. Introduction

Microtubules are cytoskeletal protein polymers formed by highly dynamic assemblies of  $\alpha$ -tubulin and  $\beta$ -tubulin heterodimers and play a crucial role in many biological processes, including mitosis, intracellular transport, exocytosis and cell division.<sup>1a</sup> Because of the role of microtubules in mitosis and cell division, they have been an important target for the development of new anticancer drugs.<sup>1b</sup> There are two major groups of these antitumor agents: microtubule stabilizers such as paclitaxel<sup>2</sup> and microtubule destabilizers (colchicine,<sup>3</sup> combretastatin A-4<sup>4</sup> and vinca alkaloids<sup>5</sup>). Most of these compounds arrest cancer cells in G2/M phases of the cell cycle and cause mitotic catastrophe and finally induce apoptosis.<sup>6</sup>

In our earlier reports,<sup>7</sup> compounds **1** and **2** were shown to exhibit good growth inhibition activity against various human tumor cell lines at the concentration of  $10^{-6}$ – $10^{-8}$  M. Compound **1** was also found to arrest cancer cells in G2/M via microtubule depolymerization and induce apoptosis via activation of caspase family.<sup>7a</sup> Comparing the structure of compound **1** with some of the common microtubule depolymerization agents, we found that the structure of compound **1** is similar to combretastatin A-4 (CA-4) and colchicine. According to our ligand docking experiment, compound **1** binds

to the  $\alpha$ - and  $\beta$ -tubulin in the same manner as colchicine. The trifluoromethylphenyl group of **1** sits into the pocket of  $\beta$ -tubulin just like the trimethoxyphenyl subunit of colchicine and the amino group of compound **1** would form hydrogen bonding with the amino acids, 179-Thr and 181-Val, of  $\alpha$ -tubulin, that is similar to the hydroxyl group of CA-4 and the carbonyl group of colchicine. (Fig. 1) However, both of the cell growth and tubulin inhibition activities of compound **1** are around 10-fold lower than that of colchicine and CA-4. As shown in Figure 1c, the distances between the amino group of **1** and the amino acids, 179-Thr and 181-Val, are 4.159 Å and 3.358 Å, respectively. They are longer than that of CA-4 and colchicine. We therefore anticipated that conversion of the amino functionality of compound **1** to the amides would shorten the distances of these hydrogen bondings and enhance the biological activities. Thus, a series of amide analogs of **1** and **2**, compounds **4a–f**, **5a–f** and **6–9**, were synthesized. These compounds were evaluated in the in vitro antitumor protocol of the NCI. They were also evaluated in the cell cycle analysis, the caspase-3, -8 and -9 colorimetric assay, microtubule depolymerization assay and Western blot analysis with apoptotic-associated proteins.

## 2. Chemistry

The synthesis of compounds **4a–f**, **5a–f** and **6–9**, are summarized in Scheme 1. Treatment of 2-(6-(2-trifluoromethylphenyl)-3(Z)-

\* Corresponding author. Tel.: +886 7 5252000x3914; fax: +886 7 5253908.  
E-mail address: [mijuwu@faculty.nsysu.edu.tw](mailto:mijuwu@faculty.nsysu.edu.tw) (M.-J. Wu).

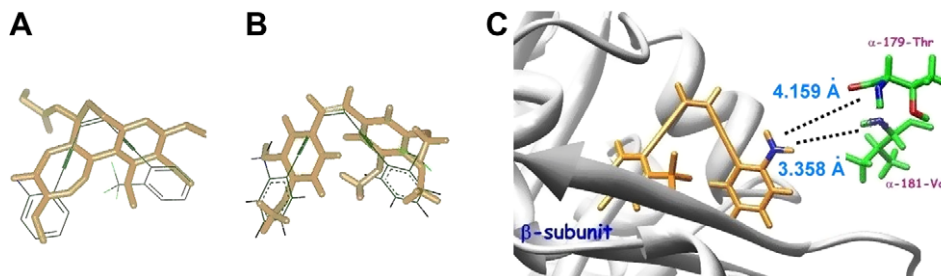
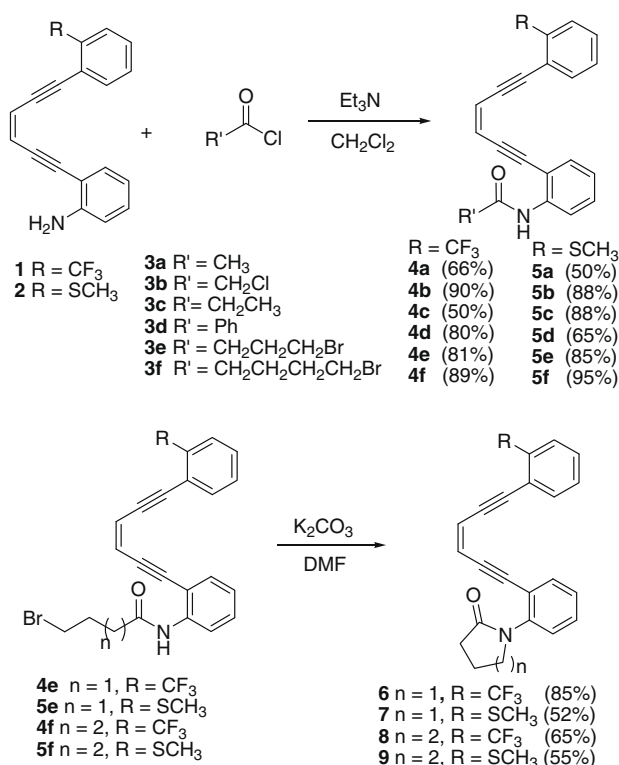


**Figure 1.** Predicted binding model of compound **2** in  $\alpha$ -,  $\beta$ -tubulin. (A) Indicate: DAMA-colchicine (gold) and compound **2** (green). (B) Indicate: CA-4 (gold) and compound **2** (green). (C) Comparison of the proposed binding mode of compound **2** with  $\alpha$ - and  $\beta$ -tubulin that are shown in a ribbon representation. Protein comes from the X-ray structure that complex with DAMA-colchicine (PDB code: 1SA0).



**Scheme 1.**

hexen-1,5-diyne)aniline (**1**)<sup>7a</sup> and 2-(6-(2-methylthiophenyl)-3(Z)-hexen-1,5-diyne)aniline (**2**)<sup>7b</sup> with various acyl chlorides **3a–f** in CH<sub>2</sub>Cl<sub>2</sub> in the presence of Et<sub>3</sub>N gave **4a–f** and **5a–f** in 50–90% yields. Compounds **4e**, **4f**, **5e** and **5f** were then converted to lactams **6–9** in 52–85% yields using K<sub>2</sub>CO<sub>3</sub> as a base and DMF as the solvent.

### 3. Results and discussion

The growth inhibition activities of compounds **4a–f**, **5a–f** and **6–9** were submitted to the National Cancer Institute for testing against a panel of approximately 60 human tumor cell lines. Details of this test system have been published by others.<sup>8</sup> Compounds **4c**, **5c**, **7** and **8** displayed a broad-spectrum inhibition activity against various cancer cell lines and the results are summarized in Table 1. Herein, we only showed some cancer cell lines for every kind of cancer, including leukemia, non-small cell lung, colon, CNS, melanoma, ovarian, renal, prostate and breast cancer. The average GI<sub>50</sub> values of these compounds are in the range of 10<sup>-7</sup>–10<sup>-6</sup> M. Of these compounds, compound **8** showed the most potent growth inhibitory activity against all tumor cell lines.

**Table 1**

The in vitro testing results of compounds **4c**, **5c**, **7** and **8**

Panel/cell line	GI <sub>50</sub> <sup>a</sup> (μM)			
	<b>4c</b>	<b>5c</b>	<b>7</b>	<b>8</b>
Leukemia-(K-562)	6.36	2.29	0.44	8.56
Leukemia-(CCRF-CEM)	2.75	0.79	0.21	1.56
Non-small cell lung cancer-(HOP-62)	10.00	2.52	5.02	0.89
Colon cancer-(HCT-15)	4.27	3.35	1.53	1.53
Colon cancer-(HCC-2998)	5.08	4.19	1.32	0.95
CNS cancer-(SNB-75)	4.76	0.63	2.34	1.61
Melanoma-(M14)	12.00	1.79	3.00	0.90
Melanoma-(UACC-62)	4.04	1.69	1.44	1.44
Ovarian cancer-(OVCAR-3)	8.87	1.79	1.03	0.87
Renal cancer-(ACHN)	30.10	4.08	10.50	2.67
Prostate cancer-(DU-145)	40.50	1.93	10.10	1.68
Breast cancer-(MDA-MB-231/ATCC)	7.92	2.17	1.19	1.16
Breast cancer-(MDA-MB-435)	1.92	0.75	0.90	0.60

Data obtained from the NCI's in vitro human tumor cell screen.

<sup>a</sup> The concentration produces 50% reduction in cell growth.

In flow cytometry assay, treatment of K-562 cells with compounds **4c**, **5c**, **7** and **8** for 24 h resulted in arrest the cell in the G2/M phase and induction of apoptosis. (Fig. 2) The percentage of G2/M phase increased from 21.1% (control) to 51.7% and 78.3% by compounds **7** and **8** at the concentration of 10 μM. At higher concentration of 50 μM, compound **8** induced the percentage of sub-G1 area is 31.57% that is 4.5 times higher than the control (7.5%). It also indicated that the induction of apoptosis by compound **8** (51.0%) is about three times higher than the lead compound **1** (19.4%) (Fig. 3).

To evaluate the relationship between the G2/M phase arrest caused by compound **8** and microtubule function, the microtubule depolymerization assay was carried out. Treatment of Hela cells with compound **8** at the concentration of 50 μM for two hours and the results is shown in Figure 4. The results indicate that compound **8** displays significant microtubule depolymerization activity just as compound **1** does. By comparing with these bioassay results, compound **8** not only shows the potency of growth inhibition activity against human tumor cell lines and the activity of microtubule depolymerization, but also shows apoptotic activity.

Caspases are the family of cysteine proteases and they mediate apoptotic pathway in mammalian.<sup>9</sup> According to the previous reports, apoptosis can be induced in either extrinsic or intrinsic pathways. Extrinsic pathway is dependent on death ligands that are stimulated by death signals, such as Fas, TRAIL or TNFα. After this process, caspase-8 was activated to trigger apoptosis. In contrast with extrinsic pathway, intrinsic pathway was caused by intracellular stresses, such as DNA damage, oncogene activation and mitotic damage.<sup>10</sup> Caspase-3, -8 and -9 in particular are the principal promoters of apoptosis. Colorimetric assays of caspase-3, -8 and -9 provided evidence of the relationship between compound **8**

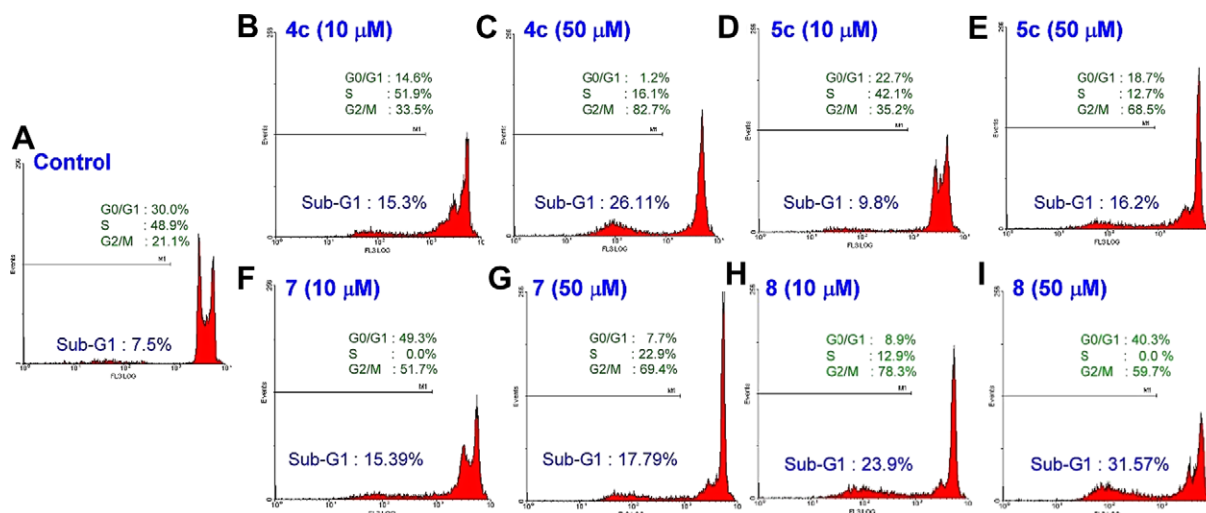


**Figure 2.** The analysis of cancer cell cycle. Leukemia (K-562 cells) was cultured with 10 μM and 50 μM of compounds **4c**, **5c**, **7** and **8** for 24 h and analyzed by flow cytometry. G0/G1, S, and G2/M individually indicate each phase and sub-G1 area refers to the portion of apoptotic cells.

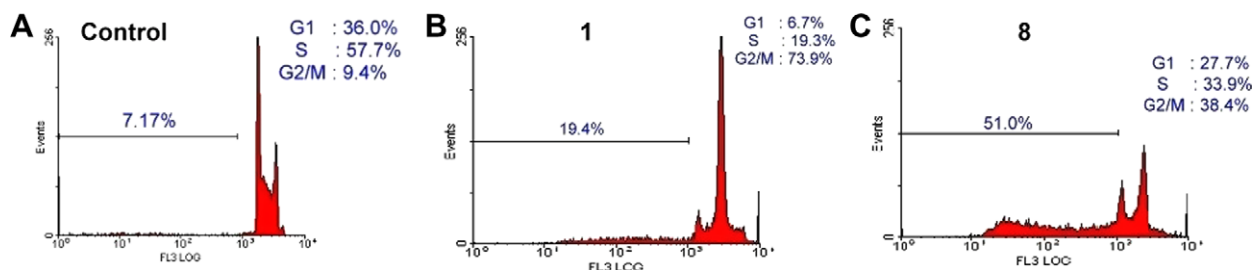


**Figure 3.** The analysis of cancer cell cycle. Compounds **1** and **8** (50 μM) treated with Leukemia (K-562 cells) for 24 h. The portion of apoptosis area: (A) control (7.17%); (B) **1** (19.4%) and (C) **8** (51.0%).

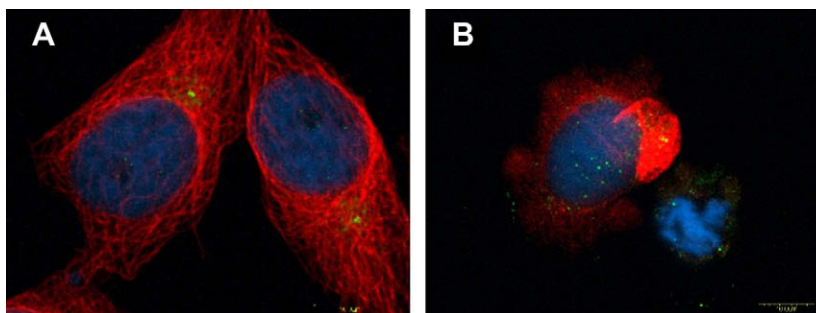


**Figure 4.** The dose effect of compound **8** on microtubules depolymerization. HeLa cells were treated with compound **8** at 37 °C in 0 μM (A) and 50 μM (B) for 2 h, respectively. Then cells were fixed and immunostained with anti-ninein (green in merged images) antibody and anti- $\alpha$ -tubulin (red in merged images) antibody and counterstained with DAPI for nucleus staining. Scale bars represent 10 μM.

and apoptosis pathways: extrinsic (relative to caspase-3 and -8) or intrinsic pathway (relative to caspase-3 and -9). As shown in Figure 5(A), compounds **1** and **8** induced caspase-3 activity in a concentration-dependent manner. But in Figure 5(B), the activity of caspase-8 was not relative to the concentrations of compound **1** or **8**. In Figure 5(C), compounds **1** and **8** can induce caspase-9 activity, particularly at the concentration of 25 μM and 50 μM. These results demonstrated that the apoptosis pathway of compounds **1** and **8** stemmed from intrinsic pathway and compound **8** showed higher caspase induction activity than **1**.

The intrinsic pathway is related to the mitochondrial function. In order to confirm the relationship of compound **8** with these apoptotic-associated proteins (Bax, Bcl-2, XIAP, Cyt.c and PARP),

compound **8** was treated with these proteins by Western blot analysis and the results are shown in Figure 6. The induced apoptosis effect of compound **8** was associated with the up-regulation of Bax and down-regulation of Bcl-2 and XIAP, as well as cytochrome c release in a concentration-dependent manner. On the other hand, caspase-3 activation was accompanied by the cleavage of PARP (Poly (ADP-ribose) polymerase).

#### 4. Conclusion

After the structure modification, we found that compound **8**, the lactam analog of compound **1**, exhibits good growth inhibition activity against human tumor cell lines and arrests cancer cell in

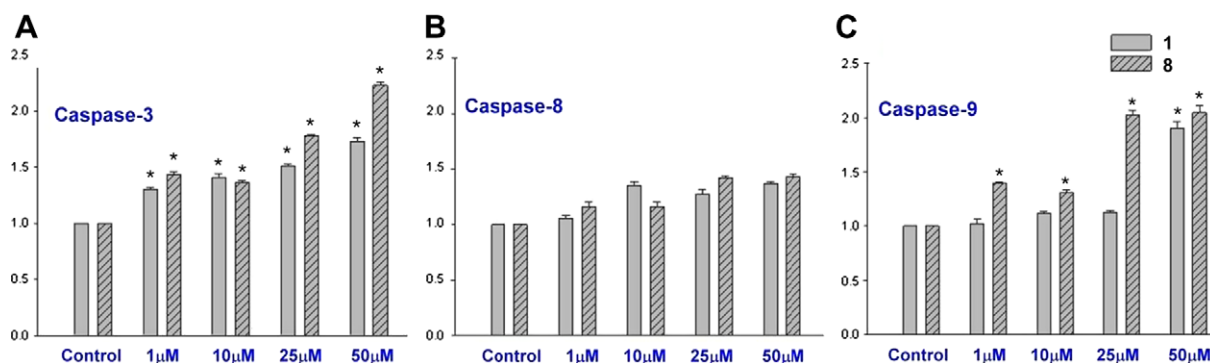


**Figure 5.** Induction of caspase-3 (A), -8 (B) and -9 (C) activity in different dose of compound 1 and 8.

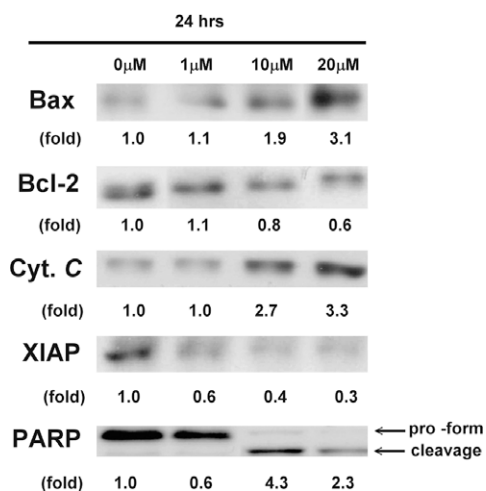


**Figure 6.** Western blot analyses of expression levels of Bax, Bcl-2, XIAP, Cyt.C and PARP. Cells were treated with different doses of compound 8 in 24 h.

the G2/M phase via microtubule depolymerization. The apoptosis mechanism of compound 8 was demonstrated through the intrinsic pathway and compound 8 showed higher caspase induction activity than 1. According to western-blotting analysis, compound 8 can up-regulate Bax, down-regulate Bcl-2 and XIAP, as well as promote cytochrome *c* release. This study provides a new lead for the development of anticancer agent. We believe that the information disclosed in this paper would have a strong impact to the development of new anticancer drugs.

## 5. Experimental section

### 5.1. Cell culture

Human leukemia K-562 cells were obtained from the American Type Culture Collection (ATCC, Manassas, VA), and human purified lymphocytes preparation was obtained from blood as described previously. Cells were maintained in RPMI 1640 medium supplemented with 10% fetal calf serum, 2 μM glutamine, and antibiotics (100 units/ml penicillin and 100 μ/ml streptomycin) at 37 °C in a humidified atmosphere of 5% CO<sub>2</sub>.

### 5.2. Cell cycle analysis

Flow cytometry was used to measure cell cycle profile and apoptosis. For cell cycle analysis, K-562 cells treated with compounds 4c, 5c, 7 and 8 (10 and 50 μM) for 24 h were harvested by centrifugation. After being washed with PBS, the cells were

fixed with ice-cold 70% ethanol for 30 min, washed with PBS, and then treated with 1 ml of 1 mg/ml of RNase A solution at 37 °C for 30 min. Cells were harvested by centrifugation at 1000 rpm for 5 min and further stained with 250 μl of DNA staining solution (10 mg of propidium iodide [PI], 0.1 mg of trisodium citrate, and 0.03 ml of Triton X-100 were dissolved in 100 ml H<sub>2</sub>O) at room temperature for 30 min in the dark. After loading 500 μl of PBS, the DNA contents of 10,000 events were measured by FACScan (Elite ESP, Beckman Coulter, Brea, CA) and the cell cycle profile was analyzed from the DNA content histograms with WinCycle software. When cells were apoptosis the containing DNA were digested by endonuclease then the sub G1 peak appear. The percentage in sub G1 were analyzed by gating on cell cycle dot blots using Windows Multiple Document Interface software (WinMDI).

### 5.3. Caspases colorimetric assay

After different treatments, K-562 cells ( $1 \times 10^6$  cells/ml) were collected and washed three times with PBS. Resuspended in 200 μl cell lysis buffer (Biovision) and incubate cells on ice for 10 min. Cell lysates were clarified by centrifugation at 18,000 g for 3 min. Transfer supernatant (cytosolic extract) to a fresh tube and keep on ice. The protein concentration in the supernatant was determined with a BCA protein assay kit (Pierce, Rockford, IL, USA), and clear lysates containing 50 μg of protein were incubated with 100 μM of enzyme-specific colorimetric substrates (Biovision) and 2X reaction buffer (Biovision) containing 10 mM DTT at 37 °C for 1 h. The activity of caspases were described as the cleavage of colorimetric substrate by measuring the absorbance at 405 nm.<sup>11</sup>

### 5.4. Immunocytochemistry and microscopy

These procedures were modified from previously described protocols.<sup>12</sup> In brief, Hela cells were grown on glass coverslips at a density of  $1 \times 10^4$  cells for 24 h. Cell cultures were rinsed several times with PBS and fixed in 4% paraformaldehyde for 5 min, permeabilized with 0.5% Triton X-100 in PBS for 5 min. Fixed cells were rinsed in PBS, and non-specific binding was blocked with 5% normal goat serum (NGS)/1% bovine serum albumin (BSA) in PBS pH 7.4 for at least 30 min at 37 °C. After a brief wash, the cells were incubated for 45 min at 37 °C with the primary antibodies diluted in the same blocking solution. After extensive washes with PBS, the cultures were then incubated with the appropriate secondary antibody conjugated to either Alexa 488 or Alexa 568 for 45 min at 37 °C. Finally, the cells were incubated for 5 min with DAPI (Roche) prior to mounting (Molecular Probes, USA). Confocal images were obtained using an OLYMPUS IX71 microscope (100x UPlanFl objective 1.3 NA) at 0.2 μm z-steps, controlled by FLUOVIEW software (Universal Imaging). All images were imported into Adobe Photoshop v7.0 for contrast manipulation.

## 5.5. Western blot analysis

Cells were harvested and extracted with lysis buffer [50 mM Tris–HCl (pH 7.5), 137 mM sodium chloride, 1 mM EDTA, 1% Nonidet P-40, 10% glycerol, 0.1 mM sodium orthovanadate, 10 mM sodium pyrophosphate, 20 mM  $\beta$ -glycerophosphate, 50 mM sodium fluoride, 1 mM phenylmethylsulfonyl fluoride, 2  $\mu$ M leupeptin, and 2  $\mu$ g/ml aprotinin]. The lysates were centrifuged at 20,000 g for 30 min and the protein concentration in the supernatant was determined with a BCA protein assay kit (Pierce, Rockford, IL, USA). Equal amounts of protein were separated by SDS-polyacrylamide gel electrophoresis and then were electrotransferred to the PVDF membrane. The membrane was blocked with a solution containing 5% nonfat dry milk TBST buffer (20 mM Tris–HCl, pH 7.4, 150 mM NaCl and 0.1% Tween 20) for 1 h and washed with TBST buffer. The indicated primary antibodies were incubated, washed, and monitored by immunoblotting using specific antibodies. These immunoreactive proteins were detected by enhanced chemiluminescence.

### 5.5.1. *N*-(2-((*Z*)-6-(2-(Trifluoromethyl)phenyl)hexa-3-en-1,5-diyndiyl)phenyl)acetamide (4a)

$^1\text{H}$  NMR ( $\text{CDCl}_3$ , 400 MHz)  $\delta$  8.40 (d, 1H,  $J$  = 8.4 Hz), 7.90 (s, 1H), 7.67 (d, 1H,  $J$  = 7.6 Hz), 7.58 (d, 1H,  $J$  = 7.6 Hz), 7.51–7.42 (m, 3H), 7.35 (td, 1H,  $J$  = 7.6, 1.2 Hz), 7.05 (t, 1H,  $J$  = 7.6 Hz), 6.37 (d, 1H,  $J$  = 11.2 Hz), 6.23 (d, 1H,  $J$  = 11.2 Hz), 1.86 (s, 3H);  $^{13}\text{C}$  NMR ( $\text{CDCl}_3$ , 100 MHz)  $\delta$  168.3, 139.0, 134.1, 131.8, 131.6, 131.4, 130.2, 128.7, 126.1, 126.0, 126.0, 123.3, 120.9, 119.7, 119.3, 119.2, 93.5, 93.1, 92.6, 92.0, 29.6; HRMS calcd for  $\text{C}_{21}\text{H}_{14}\text{F}_3\text{NO}$ , 353.1027; found, 353.1021.

### 5.5.2. *N*-(2-((*Z*)-6-(2-(Methylthio)phenyl)hexa-3-en-1,5-diyndiyl)phenyl)acetamide (5a)

$^1\text{H}$  NMR ( $\text{CDCl}_3$ , 400 MHz)  $\delta$  8.39 (d, 1H,  $J$  = 8.4 Hz), 8.15 (s, 1H), 7.48–7.29 (m, 4H), 7.13–7.03 (m, 3H), 6.24 (d, 1H,  $J$  = 10.8 Hz), 6.16 (d, 1H,  $J$  = 10.8 Hz), 2.32 (s, 3H), 1.88 (s, 3H);  $^{13}\text{C}$  NMR ( $\text{CDCl}_3$ , 100 MHz)  $\delta$  168.6, 142.1, 139.0, 131.6, 131.8, 130.0, 129.5, 124.2, 124.0, 123.7, 120.2, 119.8, 119.7, 119.2, 118.5, 94.9, 94.0, 93.3, 92.2, 24.4, 14.2; HRMS calcd for  $\text{C}_{21}\text{H}_{17}\text{NOS}$ , 331.1031; found, 331.1029.

### 5.5.3. 2-Chloro-*N*-(2-((*Z*)-6-(2-(trifluoromethyl)phenyl)hexa-3-en-1,5-diyndiyl)phenyl)acetamide (4b)

$^1\text{H}$  NMR ( $\text{CDCl}_3$ , 400 MHz)  $\delta$  9.21 (s, 1H), 8.39 (d, 1H,  $J$  = 8.0 Hz), 7.66 (d, 1H,  $J$  = 8.0 Hz), 7.60 (d, 1H,  $J$  = 7.6 Hz), 7.53–7.48 (m, 2H), 7.45–7.26 (m, 2H), 7.13 (td, 1H,  $J$  = 7.4, 1.2 Hz), 6.20 (s, 2H), 4.13 (s, 2H);  $^{13}\text{C}$  NMR ( $\text{CDCl}_3$ , 100 MHz)  $\delta$  171.2, 137.8, 134.2, 131.7, 131.4, 131.1, 130.2, 130.1, 128.5, 126.0, 125.9, 125.9, 124.3, 119.8, 119.2, 119.1, 94.1, 93.6, 91.9, 91.8, 43.0; HRMS calcd for  $\text{C}_{21}\text{H}_{13}\text{ClF}_3\text{NO}$ , 387.0638; found, 387.0636.

### 5.5.4. 2-Chloro-*N*-(2-((*Z*)-6-(2-(methylthio)phenyl)hexa-3-en-1,5-diyndiyl)phenyl)acetamide (5b)

$^1\text{H}$  NMR ( $\text{CDCl}_3$ , 400 MHz)  $\delta$  9.22 (s, 1H), 8.38 (d, 1H,  $J$  = 7.6 Hz), 7.53 (dd, 1H,  $J$  = 7.6, 1.6 Hz), 7.43–7.28 (m, 3H), 7.14–7.06 (m, 3H), 6.25 (d, 1H,  $J$  = 10.8 Hz), 6.15 (d, 1H,  $J$  = 10.8 Hz), 4.04 (s, 2H), 2.30 (s, 3H);  $^{13}\text{C}$  NMR ( $\text{CDCl}_3$ , 100 MHz)  $\delta$  164.0, 142.1, 138.0, 132.7, 132.0, 129.9, 129.3, 124.3, 124.1, 124.0, 123.7, 120.5, 119.1, 118.0, 112.9, 95.4, 94.6, 93.3, 91.4, 43.1, 14.7; HRMS calcd for  $\text{C}_{21}\text{H}_{16}\text{ClNOS}$ , 365.0641; found, 365.0635.

### 5.5.5. *N*-(2-((*Z*)-6-(2-(Trifluoromethyl)phenyl)hexa-3-en-1,5-diyndiyl)phenyl)propionamide (4c)

$^1\text{H}$  NMR ( $\text{CDCl}_3$ , 400 MHz)  $\delta$  8.43 (d, 1H,  $J$  = 8.4 Hz), 7.99 (s, 1H), 7.67 (d, 1H,  $J$  = 7.6 Hz), 7.58 (d, 1H,  $J$  = 7.6 Hz), 7.51–7.42 (m, 2H), 7.37–7.30 (m, 1H), 7.26–7.21 (m, 1H), 7.05 (td, 1H,  $J$  = 8.4, 0.8 Hz), 6.23 (s, 2H), 2.15 (t, 2H,  $J$  = 7.2 Hz), 1.98 (d, 3H,

$J$  = 7.6 Hz);  $^{13}\text{C}$  NMR ( $\text{CDCl}_3$ , 100 MHz)  $\delta$  172.0, 139.1, 134.5, 134.1, 131.7, 130.7, 129.8, 128.7, 127.8, 127.7, 125.9, 123.2, 119.6, 119.3, 119.1, 111.3, 93.6, 93.2, 92.6, 92.0, 30.6, 9.16; HRMS calcd for  $\text{C}_{22}\text{H}_{16}\text{F}_3\text{NO}$ , 367.1184; found, 367.1188.

### 5.5.6. *N*-(2-((*Z*)-6-(2-(Methylthio)phenyl)hexa-3-en-1,5-diyndiyl)phenyl)propionamide (5c)

$^1\text{H}$  NMR ( $\text{CDCl}_3$ , 400 MHz)  $\delta$  8.42 (d, 1H,  $J$  = 8.4 Hz), 8.14 (s, 1H), 7.45–7.31 (m, 4H), 7.12–7.03 (m, 3H), 6.23 (d, 1H,  $J$  = 10.8 Hz), 6.15 (d, 1H,  $J$  = 10.8 Hz), 2.30 (s, 3H), 2.18 (q, 2H,  $J$  = 6.4 Hz), 0.97 (t, 3H,  $J$  = 7.6 Hz);  $^{13}\text{C}$  NMR ( $\text{CDCl}_3$ , 100 MHz)  $\delta$  172.2, 142.1, 139.0, 132.5, 131.8, 130.1, 129.4, 124.2, 124.0, 123.7, 123.0, 121.2, 119.8, 119.2, 118.4, 95.0, 93.9, 93.3, 92.2, 30.6, 14.6, 9.57; HRMS calcd for  $\text{C}_{22}\text{H}_{19}\text{NOS}$ , 345.1187; found, 345.1189.

### 5.5.7. *N*-(2-((*Z*)-6-(2-(Trifluoromethyl)phenyl)hexa-3-en-1,5-diyndiyl)phenyl)benzamide (4d)

$^1\text{H}$  NMR ( $\text{CDCl}_3$ , 400 MHz)  $\delta$  8.85 (s, 1H), 8.66 (d, 1H,  $J$  = 8.4 Hz), 7.81 (td, 2H,  $J$  = 4.4, 1.6 Hz), 7.70–7.67 (m, 1H), 7.65–7.52 (m, 2H), 7.49–7.30 (m, 3H), 7.24–7.22 (m, 2H), 7.12 (td, 2H,  $J$  = 7.6, 0.8 Hz), 6.24 (s, 2H);  $^{13}\text{C}$  NMR ( $\text{CDCl}_3$ , 100 MHz)  $\delta$  171.1, 139.2, 134.6, 134.3, 132.1, 132.0, 131.8, 130.4, 130.3, 129.8, 128.6, 128.5, 127.9, 126.9, 125.8, 125.7, 124.1, 123.5, 119.7, 119.2, 119.1, 111.8, 94.0, 93.3, 92.5, 92.2; HRMS calcd for  $\text{C}_{26}\text{H}_{16}\text{F}_3\text{NO}$ , 415.1184; found, 415.1191.

### 5.5.8. *N*-(2-((*Z*)-6-(2-(Methylthio)phenyl)hexa-3-en-1,5-diyndiyl)phenyl)benzamide (5d)

$^1\text{H}$  NMR ( $\text{CDCl}_3$ , 400 MHz)  $\delta$  9.04 (s, 1H), 8.66 (d, 1H,  $J$  = 8.4 Hz), 7.82–7.80 (m, 2H), 7.53 (dd, 1H,  $J$  = 8, 1.6 Hz), 7.42 (td, 2H,  $J$  = 8, 1.6 Hz), 7.26–7.09 (m, 5H), 6.76 (td, 1H,  $J$  = 7.4, 0.8 Hz), 6.65 (d, 1H,  $J$  = 8.4 Hz), 6.24 (d, 1H,  $J$  = 8.4 Hz), 6.14 (d, 1H,  $J$  = 8.4 Hz), 3.56 (s, 3H);  $^{13}\text{C}$  NMR ( $\text{CDCl}_3$ , 100 MHz)  $\delta$  165.5, 159.7, 139.3, 134.1, 133.5, 131.8, 131.5, 130.4, 130.1, 128.4, 127.0, 123.4, 121.2, 120.9, 120.6, 120.3, 119.1, 117.5, 112.2, 111.5, 110.2, 95.2, 94.5, 91.7, 91.2, 55.4; HRMS calcd for  $\text{C}_{26}\text{H}_{19}\text{NOS}$ , 393.1187; found, 393.1180.

### 5.5.9. 4-Bromo-*N*-(2-((*Z*)-6-(2-(trifluoromethyl)phenyl)hexa-3-en-1,5-diyndiyl)phenyl)butanamide (4e)

$^1\text{H}$  NMR ( $\text{CDCl}_3$ , 400 MHz)  $\delta$  8.38 (d, 1H,  $J$  = 8.4 Hz), 8.00 (s, 1H), 7.69 (d, 1H,  $J$  = 0.8 Hz), 7.59–7.41 (m, 4H), 7.30–7.37 (m, 2H), 6.22 (s, 2H), 3.32 (t, 2H,  $J$  = 6.4 Hz), 2.16–2.00 (m, 4H);  $^{13}\text{C}$  NMR ( $\text{CDCl}_3$ , 100 MHz)  $\delta$  169.8, 138.7, 134.7, 134.2, 133.8, 131.9, 131.5, 131.4, 130.2, 128.7, 127.7, 126.1, 126.0, 125.9, 123.4, 119.3, 93.7, 93.2, 92.5, 92.1, 35.2, 32.6, 27.8; HRMS calcd for  $\text{C}_{23}\text{H}_{17}\text{BrF}_3\text{NO}$  ( $\text{M}^+ + \text{H}$ ), 460.0524; found, 460.0526.

### 5.5.10. 4-Bromo-*N*-(2-((*Z*)-6-(2-(methylthio)phenyl)hexa-3-en-1,5-diyndiyl)phenyl)butanamide (5e)

$^1\text{H}$  NMR ( $\text{CDCl}_3$ , 400 MHz)  $\delta$  8.43 (s, 1H), 7.46 (dd, 1H,  $J$  = 7.6, 1.6 Hz), 7.43–7.38 (m, 1H), 7.34–7.28 (m, 3H), 7.13–7.00 (m, 3H), 6.24 (d, 1H,  $J$  = 10.8 Hz), 6.18 (d, 1H,  $J$  = 10.8 Hz), 3.32 (t, 2H,  $J$  = 6.4 Hz), 2.16–2.00 (m, 4H);  $^{13}\text{C}$  NMR ( $\text{CDCl}_3$ , 100 MHz)  $\delta$  172.2, 142.2, 139.3, 132.8, 132.7, 132.4, 131.8, 130.6, 129.4, 124.2, 123.8, 122.9, 119.6, 119.4, 118.6, 95.0, 94.1, 93.4, 92.5, 27.7, 16.1, 14.8, 8.17; HRMS calcd for  $\text{C}_{23}\text{H}_{20}\text{BrNOS}$ , 437.0449; found, 437.0446.

### 5.5.11. 5-Bromo-*N*-(2-((*Z*)-6-(2-(trifluoromethyl)phenyl)hexa-3-en-1,5-diyndiyl)phenyl)pentanamide (4f)

$^1\text{H}$  NMR ( $\text{CDCl}_3$ , 400 MHz)  $\delta$  8.40 (d, 1H,  $J$  = 8.4 Hz), 7.98 (s, 1H), 7.68 (d, 1H,  $J$  = 7.6 Hz), 7.58 (d, 1H,  $J$  = 7.6 Hz), 7.52–7.43 (m, 3H), 7.35 (td, 1H,  $J$  = 8, 1.6 Hz), 7.06 (td, 1H,  $J$  = 7.6, 0.8 Hz), 6.23 (s, 2H), 3.29 (t, 2H,  $J$  = 6.0 Hz), 2.13 (t, 2H,  $J$  = 6.8 Hz), 1.88–1.60 (m, 4H);  $^{13}\text{C}$  NMR ( $\text{CDCl}_3$ , 100 MHz)  $\delta$  170.5, 138.8, 134.1, 131.7,

131.6, 131.5, 131.2, 130.2, 128.8, 126.16, 126.11, 126.06, 126.01, 124.6, 123.3, 121.9, 93.6, 93.1, 92.6, 92.1, 36.3, 32.0, 31.7, 23.6; HRMS calcd for C<sub>24</sub>H<sub>19</sub>BrF<sub>3</sub>NO, 353.1027; found, 353.1021.

#### 5.5.12. 5-Bromo-N-(2-((Z)-6-(2-(methylthio)phenyl)hexa-3-en-1,5-diynyl)phenyl)pentanamide (5f)

<sup>1</sup>H NMR (CDCl<sub>3</sub>, 400 MHz) δ 8.38 (d, 1H, J = 8.4 Hz), 8.17 (s, 1H), 7.48–7.28 (m, 4H), 7.16–7.03 (m, 3H), 6.25 (d, 1H, J = 10.8 Hz), 6.19 (d, 1H, J = 10.8 Hz), 3.23 (t, 2H, J = 6.8 Hz), 2.32 (s, 3H), 2.12 (t, 2H, J = 6.8 Hz), 1.66–1.56 (m, 4H); <sup>13</sup>C NMR (CDCl<sub>3</sub>, 100 MHz) δ 170.7, 138.9, 132.8, 132.1, 131.8, 130.0, 129.0, 124.1, 124.0, 123.6, 123.2, 120.1, 119.4, 118.5, 117.5, 94.0, 93.5, 93.0, 36.3, 33.0, 31.9, 23.7, 14.6; HRMS calcd for C<sub>24</sub>H<sub>22</sub>BrNOS, 451.0605; found, 451.0612.

#### 5.5.13. 1-(2-((Z)-6-(2-(Trifluoromethyl)phenyl)hexa-3-en-1,5-diynyl)phenyl)pyrrolidin-2-one (6)

<sup>1</sup>H NMR (CDCl<sub>3</sub>, 400 MHz) δ 7.67–7.56 (m, 3H), 7.51 (td, 1H, J = 4.4, 0.8 Hz), 7.48–7.36 (m, 3H), 7.33–7.24 (m, 1H), 6.14 (s, 2H), 3.89 (dd, 2H, J = 9.6, 7.2 Hz), 2.42 (t, 2H, J = 7.6 Hz), 2.09–2.01 (m, 2H); <sup>13</sup>C NMR (CDCl<sub>3</sub>, 100 MHz) δ 174.9, 140.2, 134.2, 133.8, 133.6, 131.5, 129.8, 129.7, 128.4, 128.3, 127.6, 127.3, 127.2, 126.0, 125.8, 120.0, 94.4, 93.1, 92.6, 91.4, 31.9, 31.4, 29.6; HRMS calcd for C<sub>23</sub>H<sub>16</sub>F<sub>3</sub>NO, 379.1184; found, 379.1192.

#### 5.5.14. 1-(2-((Z)-6-(2-(Methylthio)phenyl)hexa-3-en-1,5-diynyl)phenyl)pyrrolidin-2-one (7)

<sup>1</sup>H NMR (CDCl<sub>3</sub>, 400 MHz) δ 7.47–7.38 (m, 2H), 7.35–7.25 (m, 2H), 7.17–7.00 (m, 4H), 6.24 (d, 1H, J = 10.8 Hz), 6.17 (d, 1H, J = 10.8 Hz), 2.42 (t, 2H, J = 8.4 Hz), 2.34 (s, 3H), 2.09–2.01 (m, 4H); <sup>13</sup>C NMR (CDCl<sub>3</sub>, 100 MHz) δ 172.1, 142.1, 139.3, 132.6, 132.4, 131.7, 130.1, 129.3, 124.0, 123.7, 123.1, 121.2, 119.8, 119.6, 118.5, 94.9, 93.9, 93.3, 92.4, 29.6, 16.1, 14.7, 8.16; HRMS calcd for C<sub>23</sub>H<sub>19</sub>NOS, 357.1187; found, 357.1182.

#### 5.5.15. 1-(2-((Z)-6-(2-(Trifluoromethyl)phenyl)hexa-3-en-1,5-diynyl)phenyl)piperidin-2-one (8)

<sup>1</sup>H NMR (CDCl<sub>3</sub>, 600 MHz) δ 7.66–7.60 (m, 2H), 7.59–7.58 (m, 1H), 7.49 (td, 1H, J = 7.8, 0.6 Hz), 7.42–7.37 (m, 2H), 7.29 (td, 1H, J = 7.8, 1.2 Hz), 7.22 (dd, 1H, J = 7.8, 6.6 Hz), 6.14 (d, 1H, J = 10.8 Hz), 6.12 (d, 1H, J = 10.8 Hz), 3.70–3.50 (m, 2H), 2.47 (t, 2H, J = 6.6 Hz), 1.86–1.84 (m, 4H); <sup>13</sup>C NMR (CDCl<sub>3</sub>, 100 MHz) δ 170.0, 144.7, 134.3, 133.3, 131.4, 129.9, 128.3 (2C), 128.2 (2C), 127.4, 125.8 (2C), 121.4, 120.0, 118.9, 94.2, 92.9, 92.1, 90.5, 51.1,

32.5, 23.3, 21.3; HRMS calcd for C<sub>24</sub>H<sub>18</sub>F<sub>3</sub>NO, 393.1340; found, 393.1343.

#### 5.5.16. 1-(2-((Z)-6-(2-(Methylthio)phenyl)hexa-3-en-1,5-diynyl)phenyl)piperidin-2-one (9)

<sup>1</sup>H NMR (CDCl<sub>3</sub>, 400 MHz) δ 7.62 (dd, 1H, J = 7.6, 1.2 Hz), 7.52–7.36 (m, 2H), 7.32–7.20 (m, 3H), 7.17–7.05 (m, 2H), 6.18 (d, 1H, J = 11.2 Hz), 6.10 (d, 1H, J = 10.8 Hz), 3.70–3.61 (m, 2H), 2.52–2.47 (m, 4H), 2.39 (s, 3H), 1.84 (t, 2H, J = 2.8 Hz); <sup>13</sup>C NMR (CDCl<sub>3</sub>, 100 MHz) δ 170.2, 133.6, 132.6, 129.9, 129.7, 129.2, 129.1, 128.1, 127.3, 124.1, 124.0, 123.9, 120.8, 119.3, 118.9, 94.7, 93.8, 93.3, 91.0, 51.1, 32.5, 23.4, 21.3, 14.9; HRMS calcd for C<sub>24</sub>H<sub>21</sub>NOS, 371.1344; found, 371.1337.

#### Acknowledgments

We would like to thank the National Science Council of the Republic of China for the financial support and National Institutes of Health (National Cancer Institute) for the cytotoxicity screening.

#### Supplementary data

Supplementary data associated with this article can be found, in the online version, at [doi:10.1016/j.bmc.2009.09.042](https://doi.org/10.1016/j.bmc.2009.09.042).

#### References and notes

- (a) Jordan, M. A.; Wilson, L. *Curr. Opin. Cell Biol.* **1998**, *10*, 123; (b) Jordan, M. A.; Wilson, L. *Nat. Rev. Cancer* **2004**, *4*, 253.
- Schiff, P. B.; Fant, J.; Horwitz, S. B. *Nature* **1979**, *277*, 665.
- Li, Q.; Sham, H.; Rosenberg, S. *Ann. Rep. Med. Chem.* **1999**, *34*, 139.
- Nam, N. H. *Curr. Med. Chem.* **2003**, *10*, 1697.
- Jordan, M. A.; Hadfield, J. A.; Lawrence, N. J.; McGown, A. T. *Med. Res. Rev.* **1998**, *18*, 259.
- Mahboobi, S.; Pongratz, H.; Hufsky, H.; Hockemeyer, J.; Frieser, M.; Lyssenko, L.; Paper, D. H.; Bürgermeister, J.; Böhmer, F. D.; Fiebig, H. H.; Burger, A. M.; Baasner, S.; Beckers, T. *J. Med. Chem.* **2001**, *44*, 4535.
- (a) Lo, Y. H.; Lin, C. C.; Lin, C. F.; Lin, Y. T.; Duh, T. H.; Hong, Y. R.; Yang, S. H.; Lin, S. R.; Yang, S. C.; Chang, L. S.; Wu, M. J. *J. Med. Chem.* **2008**, *51*, 2682; (b) Lin, C. F.; Lo, Y. H.; Hsieh, M. C.; Chen, Y. H.; Wang, J. J.; Wu, M. J. *Bioorg. Med. Chem.* **2005**, *13*, 3565.
- Boyd, M. R.; Paull, K. D. *Drug Dev. Res.* **1995**, *34*, 91.
- Horvitz, H. R. *ChemBioChem* **2003**, *4*, 697.
- Daniel, P. T.; Koert, U.; Schuppan, J. *Angew. Chem., Int. Ed.* **2006**, *45*, 872.
- Wu, Z. Z.; Chien, C. M.; Yang, S. H.; Lin, Y. H.; Hu, X. W.; Lu, Y. J.; Wu, M. J.; Lin, S. R. *Mol. Cell Biol.* **2006**, *292*, 99.
- Lin, C. C.; Cheng, T. S.; Hsu, C. M.; Wu, C. H.; Chang, L. S.; Shen, Z. S.; Yeh, H. M.; Chang, L. K.; Howng, S. L.; Hong, Y. R. *Cell Cycle* **2006**, *5*, 2517.